Electronic Supplementary Material (ESI) for Physical Chemistry Chemical Physics.

Elucidation of the key role of isomerization in the self-assembly and luminescence properties of AIEgens

Hui Wang,[a] Junfang Yang[a] and Xiaoyan Zheng *[ab]

[a]Key Laboratory of Cluster Science of Ministry of Education, Beijing Key laboratory of Photoelectronic/Electro-photonic Conversion Materials, Key Laboratory of Medicinal Molecule Science and Pharmaceutics Engineering of Ministry of Industry and Information Technology, School of Chemistry and Chemical Engineering, Beijing Institute of Technology, Beijing, 100081, China.

[b]Guangdong Provincial Key Laboratory of Luminescence from Molecular Aggregates (South China University of Technology), Guangzhou, 510640, China.

*E-mail: xiaoyanzheng@bit.edu.cn.

Contents

I. Supplementary Chart S1-S2 and Figures S1-S9

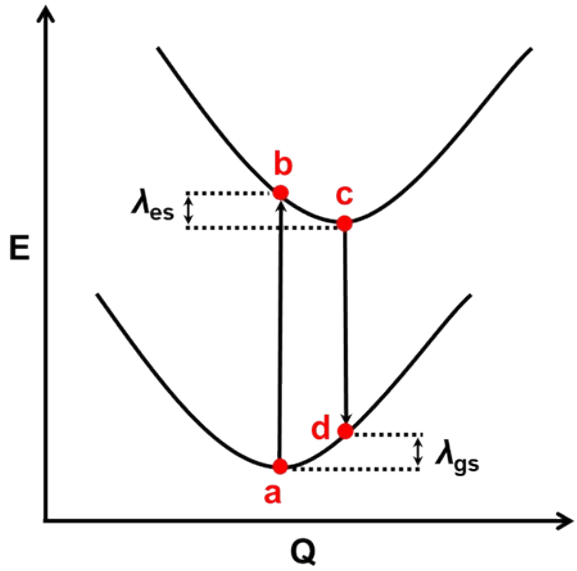

Chart S1. Schematic representation of the AP. Q refers to the nuclear configuration.

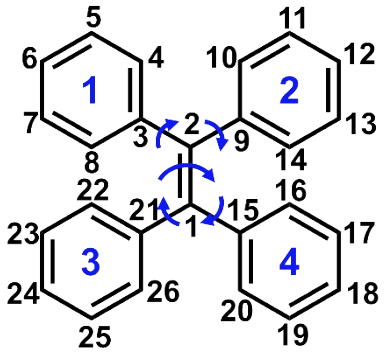

Chart S2. The chemical structure of QM region of QM/MM model in this work. The key structral parameters related to photophysical properties were also shown.

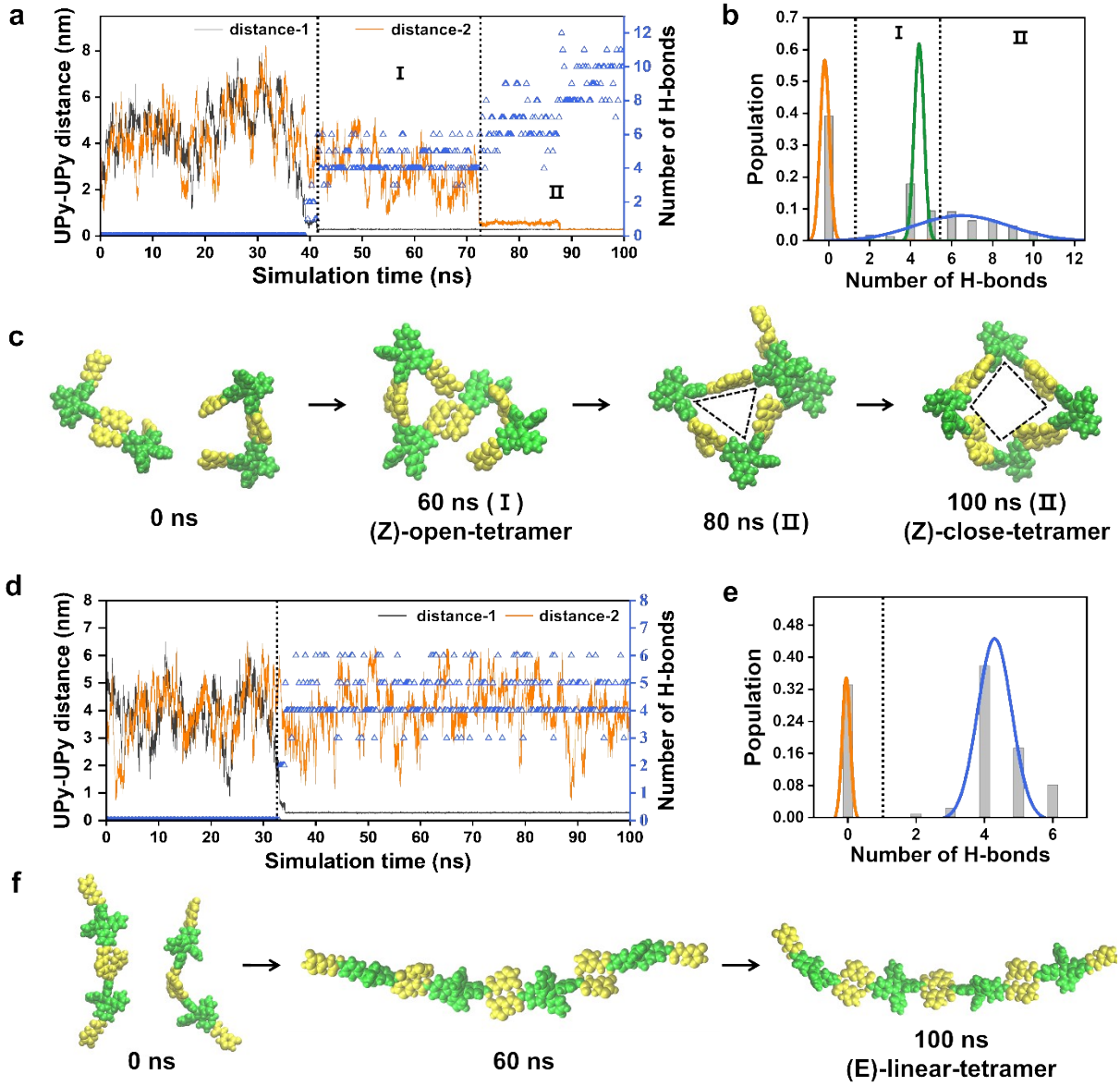

Fig. S1 (a) and (d) The distance evolution and the number of intermolecular H-bonds among unoccupied UPy moieties of (Z)-TPE-UPy and (E)-TPE-UPy at different stage of tetramer formation process. (b) and (E) Population of number of intermolecular H-bonds at different stage of (Z)- and (E)-TPE-UPy tetramer formation. (c) and (f) Representative snapshots extracted from MD trajectories of (Z)- and (E)-TPE-UPy tetramer formation. The TPE and UPy motifs are shown in green and yellow, respectively. The alkyl groups of UPy and chloroform solvents are not shown for clarity.

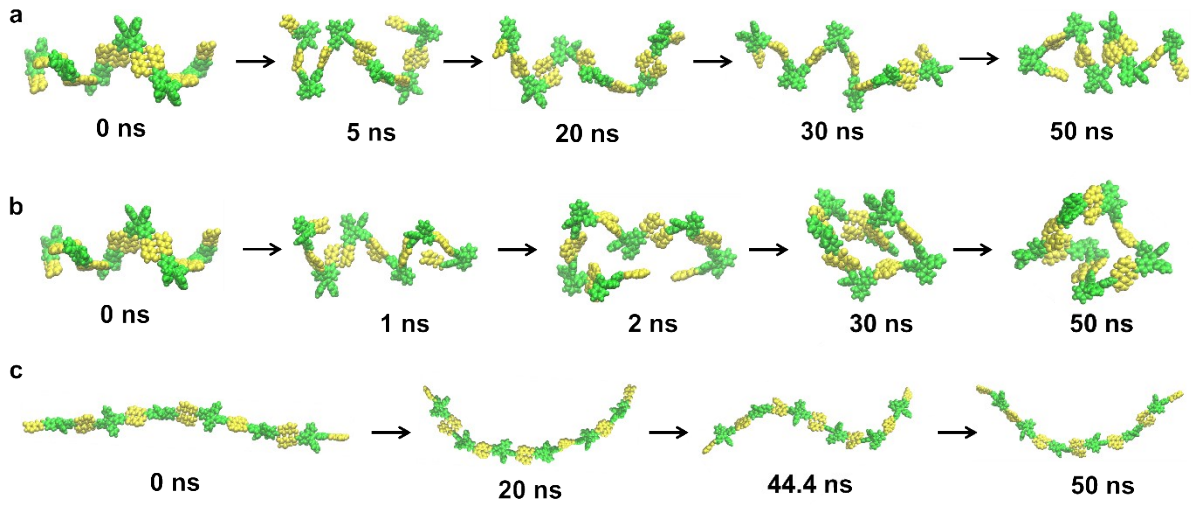

Fig. S2 The evolution of (a) (Z)-open-hexamer, (b) (Z)-close-hexamer and (c) (E)-linear-hexamer assembles presented by the representative snapshots of extracted from MD trajectories in chloroform. The TPE and UPy motifs are shown in green and yellow, respectively. The alkyl groups of UPy and chloroform solvents are not shown for clarity.

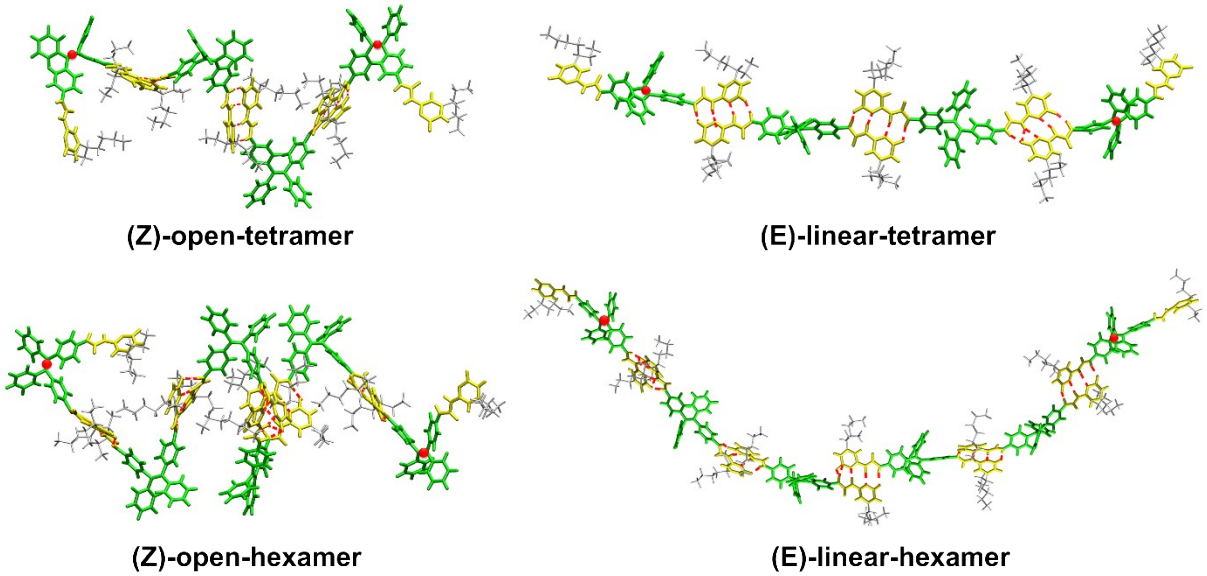

Fig. S3 Typical conformations of typical chain-like tetramers and hexamers extracted from MD trajectories. The positions of center-of-mass (COM) distance definition are marked by red dots.

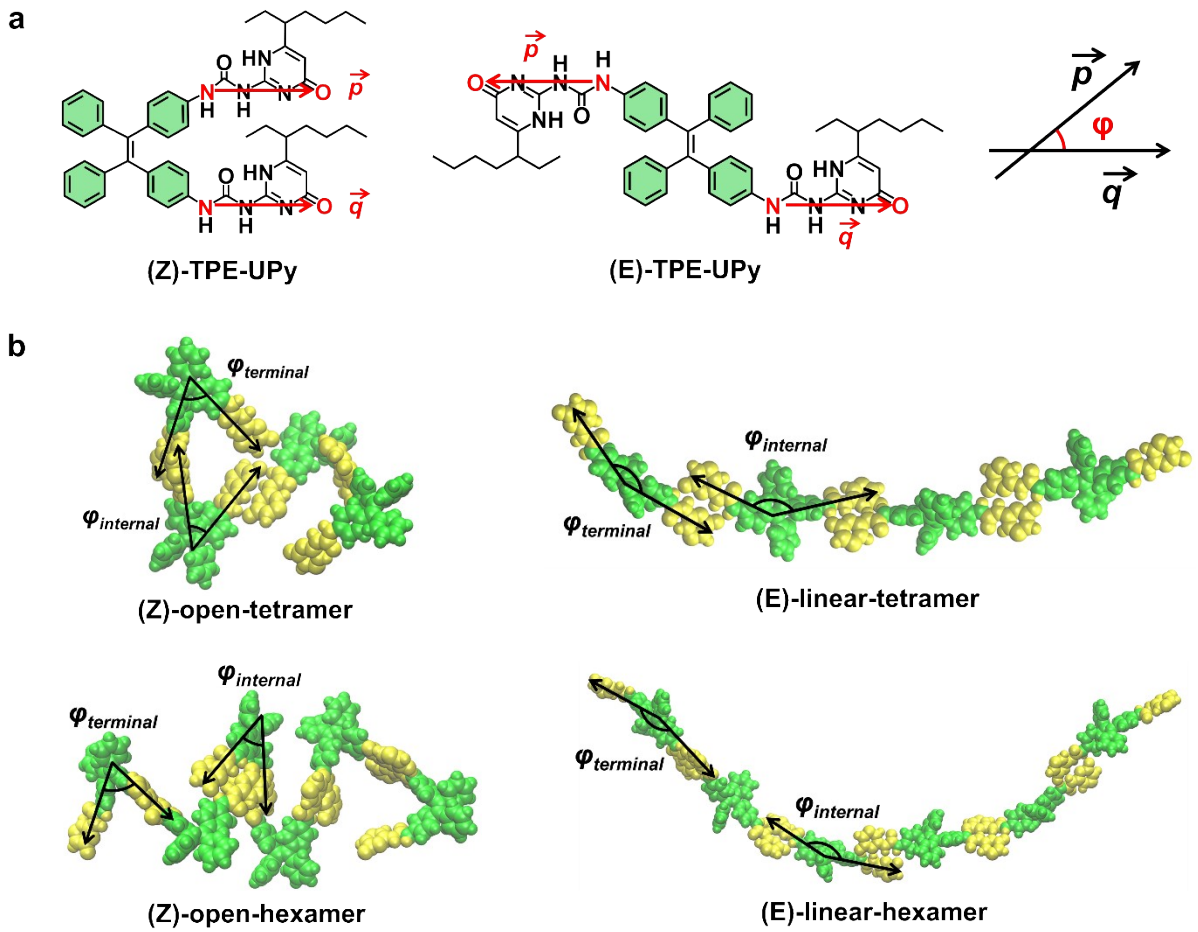

Fig. S4 (a) Definitions of two representative angles used to describe the conformational changes of both tetramers and hexamers. Two vectors $\vec{p}$ and $\vec{q}$, respectively, represent vectors connecting one nitrogen and one oxygen atoms marked in red. The included angle between $\vec{p}$ and $\vec{q}$ is defined as φ. (b) Two representative angles ($\varphi_{terminal}$ and $\varphi_{internal}$) at the terminus and the internal part of each (Z)-open-tetramer/hexamer or (E)-linear-tetramer/hexamer, respectively.

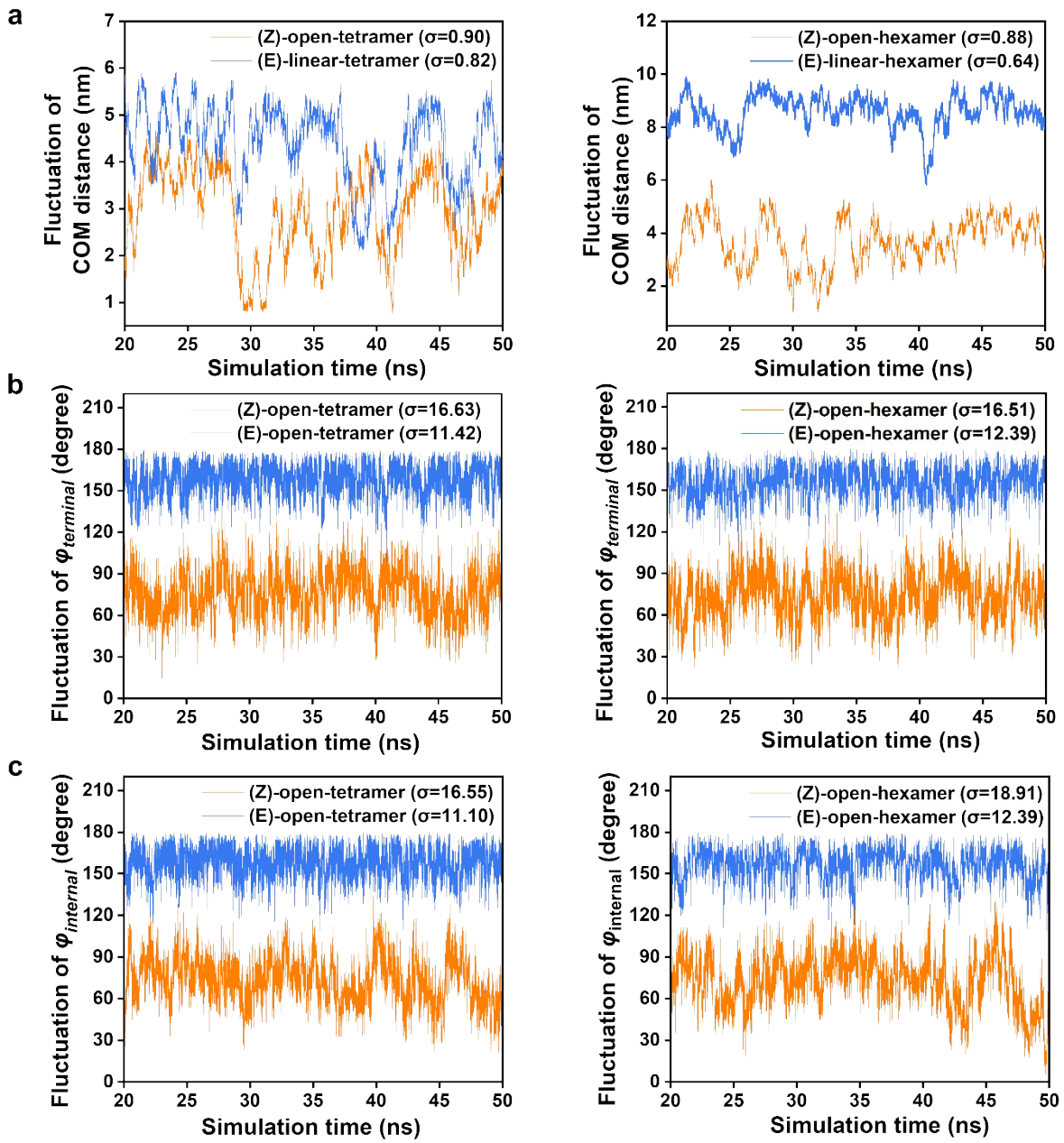

Fig. S5 The evolution of (a) COM distance and (b-c) two representative angles $\varphi_{terminal}$ and $\varphi_{internal}$ of equilibrated tetramers and hexamers as a function of simulation time. The corresponding standard deviations (σ) are shown above.

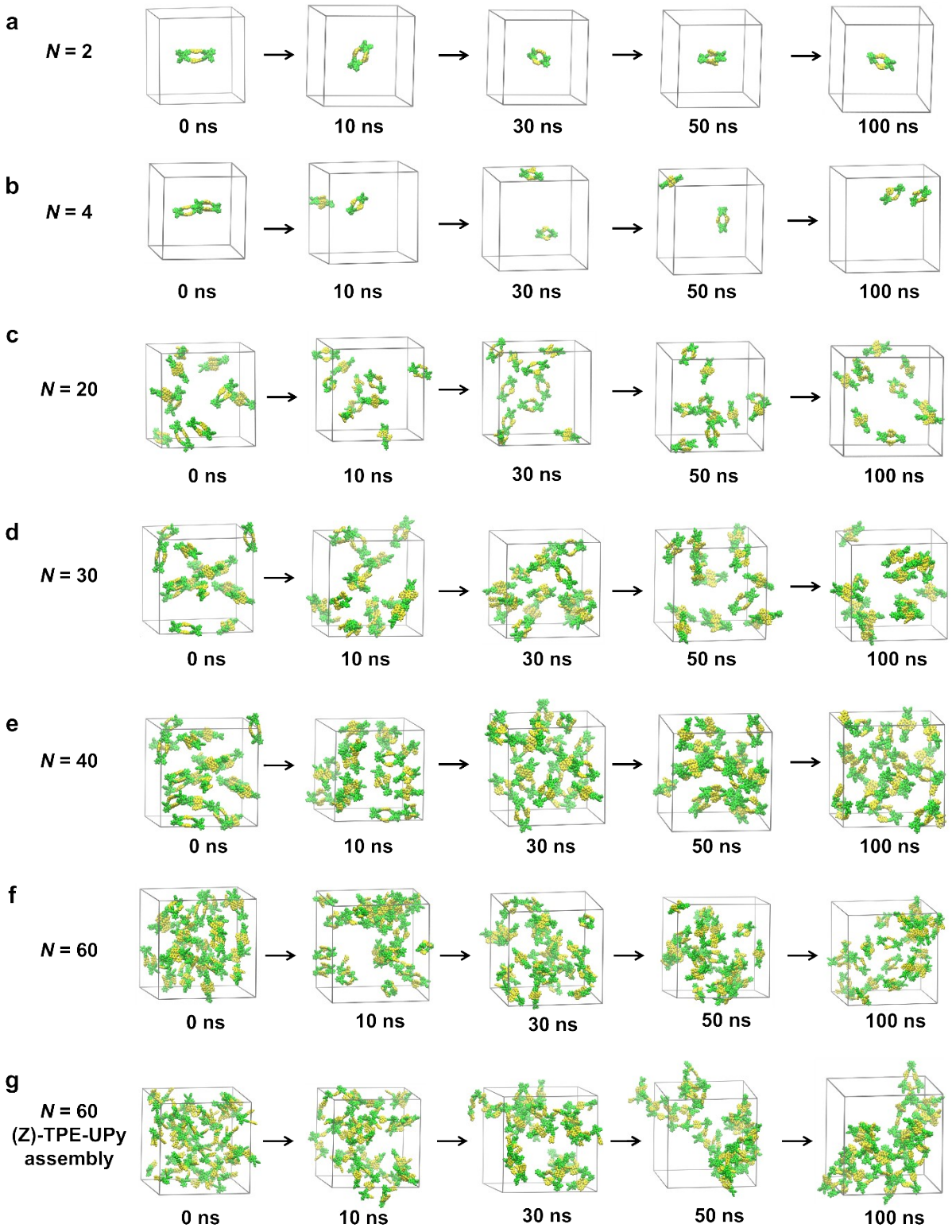

Fig. S6 The evolution of (Z)-close-dimer assemblies at different concentrations and "(Z)-TPE-UPy assembly" by the representative snapshots extracted from MD trajectories in chloroform.

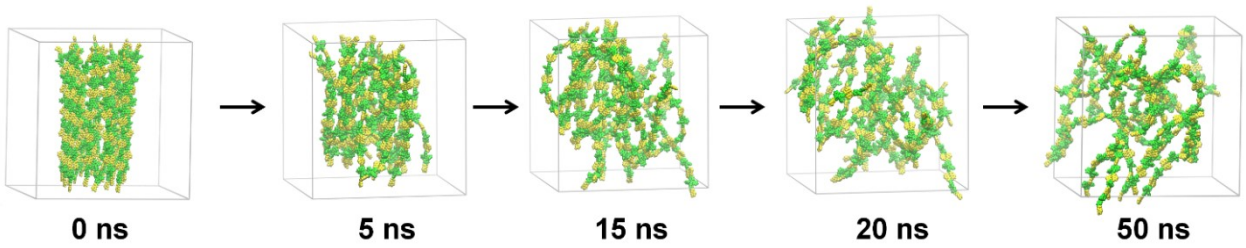

Fig. S7 The evolution of "(E)-TPE-UPy assembly" shown by representative snapshots extracted from MD trajectories in chloroform.

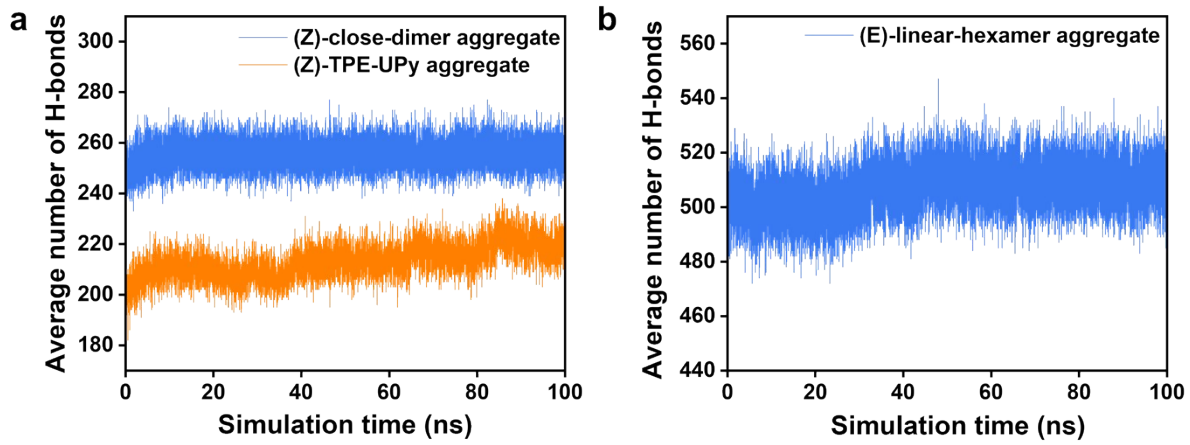

Fig. S8 Evolution of number of intermolecular H-bonds as a function of time in three typical aggregates.

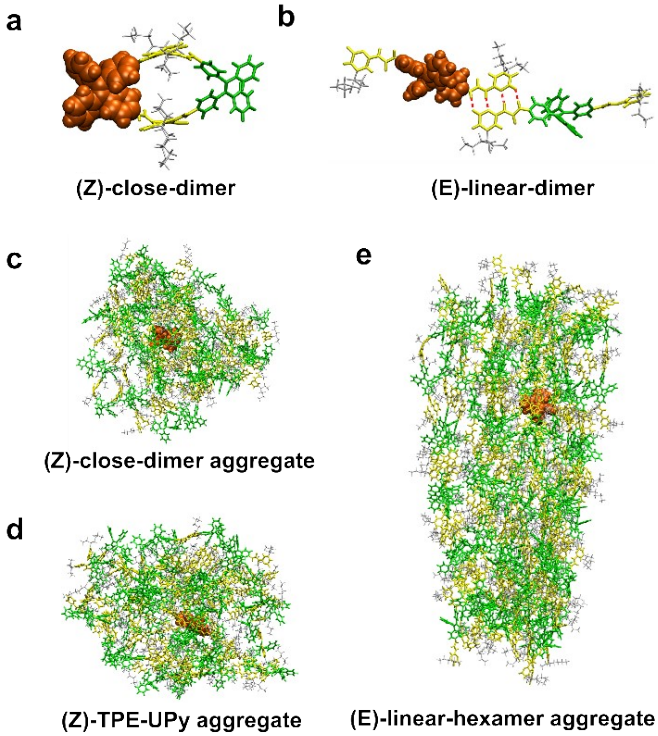

Fig. S9 The QM/MM models for the representative nanostructures, including two dimers and three typical aggregates, including (a) (Z)-close-dimer and (b) (E)-linear-dimer, (c) (Z)-close-dimer aggregate, (d) (Z)-TPE-UPy aggregate and (e) (E)-linear-hexamer aggregate. For each system, the TPE moiety in orange is selected as the high-layer QM region and treated at the M06-2X/6-311G* level.

II. Supplementary Tables S1-S8

Table S1 Selected bond lengths (in Å), bond angles (in degree), and dihedral angles (in degree) of (Z)-close-dimer at S_0 and S_1 minimum and the difference between S_0 and S_1. The definition of structral parameters are shown in Chart S2.

structural parameters		(Z)-close-dimer		
		S_0	S_1	$\|S_0-S_1\|$
bond lengths				
	C_1-C_2	1.354	1.465	0.102
	C_2-C_3	1.490	1.442	0.048
	C_2-C_9	1.491	1.444	0.047
	C_1-C_{15}	1.489	1.443	0.046
	C_1-C_{21}	1.490	1.444	0.046
bond angles				
	C_1-C_2-C_3	123.2	118.9	4.3
	C_1-C_2-C_9	122.0	118.2	3.8
	C_2-C_1-C_{15}	121.8	117.9	3.9
	C_2-C_1-C_{21}	122.9	118.7	4.2
dihedral angles				
D_1	C_1-C_2-C_3-C_4	136.2	155.4	19.2
D_2	C_1-C_2-C_9-C_{10}	129.9	147.6	17.7
D_3	C_2-C_1-C_{15}-C_{16}	-48.9	-22.7	26.2
D_4	C_2-C_1-C_{21}-C_{22}	-46.2	-21.0	25.2
D_5	C_3-C_2-C_1-C_{15}	168.0	124.9	43.1

Table S2 Selected bond lengths (in Å), bond angles (in degree), and dihedral angles (in degree) of (Z)-close-dimer aggregate at S_0 and S_1 minimum and the difference between S_0 and S_1.

structural parameters		(Z)-close-dimer aggregate		
		S_0	S_1	$\|S_0-S_1\|$
bond lengths				
	C_1-C_2	1.365	1.461	0.096
	C_2-C_3	1.493	1.444	0.049
	C_2-C_9	1.498	1.453	0.045
	C_1-C_{15}	1.492	1.459	0.033
	C_1-C_{21}	1.486	1.440	0.046
bond angles				
	C_1-C_2-C_3	124.2	123.6	0.6
	C_1-C_2-C_9	119.8	118.5	1.3
	C_2-C_1-C_{15}	118.9	118.1	0.8
	C_2-C_1-C_{21}	123.6	122.3	1.3
dihedral angles				
D_1	C_1-C_2-C_3-C_4	156.5	157.4	0.9
D_2	C_1-C_2-C_9-C_{10}	137.6	141.1	3.5
D_3	C_2-C_1-C_{15}-C_{16}	-46.4	-35.6	10.8
D_4	C_2-C_1-C_{21}-C_{22}	-44.1	-25.9	18.2
D_5	C_3-C_2-C_1-C_{15}	161.9	153.2	8.7

Table S3 Selected bond lengths (in Å), bond angles (in degree), and dihedral angles (in degree) of (Z)-TPE-UPy aggregate at S_0 and S_1 minimum and the difference between S_0 and S_1.

structural parameters		(Z)-TPE-UPy aggregate		
		S_0	S_1	$\|S_0-S_1\|$
bond lengths				
	C_1-C_2	1.357	1.455	0.098
	C_2-C_3	1.493	1.454	0.039
	C_2-C_9	1.491	1.451	0.04
	C_1-C_{15}	1.487	1.450	0.037
	C_1-C_{21}	1.492	1.445	0.047
bond angles				
	C_1-C_2-C_3	118.8	117.3	1.5
	C_1-C_2-C_9	124.1	122.4	1.7
	C_2-C_1-C_{15}	123.4	122.5	0.9
	C_2-C_1-C_{21}	123.9	122.1	1.8
dihedral angles				
D_1	C_1-C_2-C_3-C_4	127.4	137.7	10.3
D_2	C_1-C_2-C_9-C_{10}	156.3	160.0	3.7
D_3	C_2-C_1-C_{15}-C_{16}	-57.7	-43.4	14.3
D_4	C_2-C_1-C_{21}-C_{22}	-38.3	-26.3	12
D_5	C_3-C_2-C_1-C_{15}	161.4	148.9	12.5

Table S4 Selected bond lengths (in Å), bond angles (in degree), and dihedral angles (in degree) of (E)-linear-dimer at S_0 and S_1 minimum and the difference between S_0 and S_1.

structural parameters		(E)-linear-dimer		
		S_0	S_1	$\lvert S_0-S_1\rvert$
bond lengths				
	C_1-C_2	1.353	1.458	0.105
	C_2-C_3	1.489	1.446	0.039
	C_2-C_9	1.484	1.450	0.034
	C_1-C_{15}	1.494	1.454	0.04
	C_1-C_{21}	1.484	1.445	0.039
bond angles				
	C_1-C_2-C_3	123.7	120.4	3.3
	C_1-C_2-C_9	120.5	119.3	1.2
	C_2-C_1-C_{15}	122.7	118.9	3.8
	C_2-C_1-C_{21}	122.8	121.7	1.1
dihedral angles				
D_1	C_1-C_2-C_3-C_4	136.2	151.3	15.1
D_2	C_1-C_2-C_9-C_{10}	127.1	140.9	13.8
D_3	C_2-C_1-C_{15}-C_{16}	-49.5	-30.2	19.3
D_4	C_2-C_1-C_{21}-C_{22}	-47.6	-24.8	22.8
D_5	C_3-C_2-C_1-C_{15}	170.5	145.0	25.5

Table S5 Selected bond lengths (Å), bond angles (degree), and dihedral angles (degree) of (E)-linear-hexamer aggregate at S_0 and S_1 minimum and the difference between S_0 and S_1

structural parameters		(E)-linear-hexamer aggregate		
		S_0	S_1	$\|S_0-S_1\|$
bond lengths				
	C_1-C_2	1.354	1.454	0.1
	C_2-C_3	1.498	1.463	0.035
	C_2-C_9	1.491	1.442	0.049
	C_1-C_{15}	1.492	1.442	0.05
	C_1-C_{21}	1.487	1.456	0.031
bond angle				
	C_1-C_2-C_3	122.1	119.9	2.2
	C_1-C_2-C_9	124.2	123.4	0.8
	C_2-C_1-C_{15}	125.1	123.2	1.9
	C_2-C_1-C_{21}	123.0	121.0	2.0
dihedral angle				
D_1	C_1-C_2-C_3-C_4	128.2	134.5	6.3
D_2	C_1-C_2-C_9-C_{10}	148.9	151.4	2.5
D_3	C_2-C_1-C_{15}-C_{16}	-61.5	-30.1	31.4
D_4	C_2-C_1-C_{21}-C_{22}	-46.9	-36.4	10.5
D_5	C_3-C_2-C_1-C_{15}	174.9	165.4	9.5

Table S6 The extracted key dihedral angles (in degree) of two representative dimers: (Z)-close-dimer and (E)-linear-dimer, and three assembled aggregates: (Z)-close-dimer aggregate, (Z)-TPE-UPy aggregate, (E)-linear-hexamer aggregate, respectively. S_0, S_1 and $|S_0-S_1|$ represent the geometric parameters extracted from the ground, excited states and the difference between them, respectively. The definition of key dihedral angles is shown in Chart 1.

	(Z)-close-dimer			(Z)-close-dimer aggregate			(Z)-TPE-UPy aggregate			(E)-linear-dimer			(E)-linear-hexamer aggregate		
	S_0	S_1	$\Delta\|S_0-S_1\|$	S_0	S_1	$\Delta\|S_0-S_1\|$	S_0	S_1	$\Delta\|S_0-S_1\|$	S_0	S_1	$\Delta\|S_0-S_1\|$	S_0	S_1	$\Delta\|S_0-S_1\|$
D_1	136.2	155.4	19.2	156.5	157.4	0.9	127.4	137.7	10.3	136.2	151.3	15.1	128.2	134.5	6.3
D_2	129.9	147.6	17.7	137.6	141.1	3.5	156.3	160.0	3.7	127.1	140.9	13.8	148.9	151.4	2.5
D_3	-48.9	-22.7	26.2	-46.4	-35.6	10.8	-57.7	-43.4	14.3	-49.5	-30.2	19.3	-61.5	-30.1	31.4
D_4	-46.2	-21.0	25.2	-44.1	-25.9	18.2	-38.3	-26.3	12	-47.6	-24.8	22.8	-46.9	-36.4	10.5
D_5	168.0	124.9	43.1	161.9	153.2	8.7	161.4	148.9	12.5	170.5	145.0	25.5	174.9	165.4	9.5

Table S7 Calculated vertical excitation energy (ΔE_{vert}), electronic dipole moment (EDM), oscillator strength (f), the assignment for S_1 of TPE and radiative decay rate constant (k_r).

S_1	ΔE_{vert}	EDM	f	assignment	k_r (10^7)
(Z)-close-dimer	1.94 eV/638 nm	5.23 D	0.2017	HOMO→LUMO (100%)	3.29
(Z)-close-dimer aggregate	2.57 eV/482 nm	5.17 D	0.2604	HOMO→LUMO (99.4%)	7.46
(Z)-TPE-UPy aggregate	2.61 eV/474 nm	5.55 D	0.3049	HOMO→LUMO (99.3%)	9.01
(E)-linear-dimer	2.47 eV/502 nm	5.15 D	0.2485	HOMO→LUMO (99.6%)	6.58
(E)-linear-hexamer aggregate	2.72 eV/456 nm	5.03 D	0.2604	HOMO→LUMO (98.6%)	8.36

Table S8 Reorganization energy of each system calculated adiabatic potential method.

	λ_{gs} (eV)	λ_{es} (eV)	λ (eV)
(Z)-close-dimer	1.14	0.93	2.07
(Z)-close-dimer aggregate	0.52	0.57	1.09
(Z)-TPE-UPy aggregate	0.59	0.60	1.19
(E)-linear-dimer	0.74	0.81	1.53
(E)-linear-hexamer aggregate	0.67	0.73	1.40